Applied Catalysis B: Environmental 84 (2008) 363–371

Contents lists available at ScienceDirect

Applied Catalysis B: Environmental

journal homepage: www.elsevier.com/locate/apcatb

Study on reuse of metal oxide-promoted sulphated zirconia in acylation reactions

Michela Signoretto [a,b,*], Antonella Torchiaro [a], Anna Breda [a], Francesco Pinna [a,b], Giuseppina Cerrato [c,d], Claudio Morterra [c,d]

[a] Chemistry Department, University Ca'Foscari, Calle larga S. Marta, 2137 I-30123 Venezia, Italy
[b] INSTM Consortium Firenze, UdR Venezia, Italy
[c] Department of Chemistry IFM – NIS Centre of Excellence, University of Torino, Via P. Giuria, 7 I-10125 Torino, Italy
[d] INSTM Consortium Firenze, UdR Torino, Italy

ARTICLE INFO

Article history:
Received 28 January 2008
Received in revised form 4 April 2008
Accepted 12 April 2008
Available online 20 April 2008

Keywords:
Sulphated zirconia
Friedel-Crafts acylation
Fine chemicals
Catalyst regeneration

ABSTRACT

A series of sulphated zirconia samples (SZ) promoted with Al_2O_3, Ga_2O_3, and Fe_2O_3 were synthesized by co-precipitation at constant pH and aged under reflux conditions. Structural, surface and catalytic properties of the samples were investigated using N_2 adsorption/desorption, thermal analysis, *in-situ* FTIR spectroscopy, TPR–MS and EGA–MS measurements. The catalytic performance of promoted SZ in anisole acylation has been investigated. Promotion by either Fe_2O_3 or Ga_2O_3 was found to increase the catalytic activity (yield) after recycle of catalysts with respect un-promoted sample, whereas promotion by Al_2O_3 was observed to increase the conversion but not the yield. It is worth noting that all systems present high selectivity to the *p*-metoxyacetophenone product.

1. Introduction

Liquid-phase reactions, such as Friedel-Crafts acylation [1], are important unit processes for the preparation of many industrially valuable chemicals.

In recent years, increasing restrictions related to the use of traditional stoichiometric and conventional homogenous catalytic processes have been introduced because of their inherent problems such as cost, separation, handling, waste disposal, etc. [2]. Friedel-Crafts acylation is usually catalyzed by Lewis acids ($AlCl_3$, $FeCl_3$, BF_3 ...) or Brønsted acids (HF, H_2SO_4 ...). Their replacement by heterogeneous catalysts is a research topic of high interest [3–5]. Modern processes are, in fact, based on solid acids. Rhodia company (Courebevoie Cedex France), for example, is operating an industrial process for the acylation of anisole to para-acetylanisole using a zeolite-like catalyst [6]. This fixed-bed technology process is a breakthrough in the field, as it enables a considerable simplification of the process, an increase in para selectivity, and thus a reduction of the operating costs and a dramatic reduction of effluent volume. The principles of this process have been extended to the production of acetoveratrole [7]. The main drawback related to the use of zeolites is their deactivation, due to a consecutive reaction of the product with either reagents or other product molecules to form heavy by-products that remain on the catalyst [8,9]. By-products can also block the accessibility of the reactants to the catalyst micropores. In this context, sulphated zirconia (SZ) could be a better catalyst than zeolites in such reactions, due to its mesopores system which could avoid deactivation.

Recently, Jana [10] reported a new type of catalysts for Friedel-Crafts benzylation reaction. These novel red-ox metal-containing solid catalysts are very active/selective in the benzylation process.

In the present study, acylation of anisole with acetic anhydride has been investigated over Al-, Ga- and Fe-promoted SZ catalysts, and compared with unpromoted SZ systems.

Aim of this contribution is to investigate the influence of the promoters on the catalytic performances of the materials and in their possible reuse after regeneration.

2. Experimental

2.1. Catalysts synthesis

SZ samples doped with M^{3+}-oxides were synthesized by a precipitation method at constant pH, as reported elsewhere [11,12]. Briefly, a solution containing the metal cations (ZrO^{2+}

* Corresponding author. Tel.: +390 41 2348650; fax: +390 41 2348517.
E-mail address: miky@unive.it (M. Signoretto).

0926-3373/$ – see front matter © 2008 Elsevier B.V. All rights reserved.
doi:10.1016/j.apcatb.2008.04.014

Table 1
N2 physisorption and sulphates concentration data for all samples

Sample label	Surface area BET (m^2/g)		Pore volume (cm^3/g)	SO_4 wt.%		SO_4/nm^2	
	Fresh	After regeneration	Fresh	Fresh	After regeneration	Fresh	After regeneration
SZ	118	106	0.17	4.0	3.3	2.1_2	1.9_5
SZA	104	93	0.20	4.3	3.6	2.5_9	2.4_2
SZG	125	112	0.17	4.1	3.3	2.0_6	1.8_5
SZF	144	128	0.26	4.8	4.0	2.0_8	1.9_6

$ZrOCl_2{\cdot}8H_2O$ (Fluka>+98%) and a dosed amount (3 mol%) of the other metal ion, Al^{3+}, Ga^{3+}, or Fe^{3+}) ($M(NO_3)_3{\cdot}9H_2O$ (Aldrich +98%), was added dropwise under stirring to a fixed volume of water basified at pH 8 with a concentrated ammonia solution. As the precipitation of metal hydroxides tends to cause a pH dropping down, the addition of ammonia is useful to keep it constant within the range of ±0.2 pH units during the entire precipitation step.

Precipitated hydroxides were stirred for 30 min and subsequently aged for 42 h at 90 °C under reflux conditions [13–15]. Aged hydroxides were washed with water until free from chloride ions (negative $AgNO_3$ test) and dried at 110 °C for 20 h. Dried hydroxides were impregnated with a $(NH_4)_2SO_4$ solution by the incipient wetness method, to give a nominal 8 wt.% $SO_4^{=}$, and dried again at 110 °C for 20 h. Sulphated hydroxides were finally calcined at 650 °C in flowing air for 3 h. (see Table 1).

Four catalysts were prepared and they were labelled SZM, where SZ stands for sulphated zirconia, and M indicates the doping metal (Al^{3+}, Ga^{3+}, Fe^{3+}). For instance, the zirconia catalyst doped with Al_2O_3, impregnated and calcined, is referred to as SZA.

2.2. Catalysts characterization

Surface area and pore size distribution were obtained from N_2 adsorption/desorption isotherms at −196 °C (Micromeritics ASAP 2010 Analyser). Surface area was calculated by the BET equation [16]. Pore size distribution curves were determined by the BJH method applied to the adsorption isotherm branch [17].

X-ray powder diffraction patterns were measured on a Philips PW 1820/00 diffractometer, equipped with a diffracted-beam graphite monochromator, using the CuKα radiation from a sealed X-ray tube.

TPR experiments were carried out in a home-made apparatus with a 5% H_2/Ar gas mixture (40 cc/min). H_2 uptake was monitored by a Gow-Mac thermal conductivity detector (TCD), interfaced to a computer for data collection and analysis. To prevent H_2O interference in the TCD, a $Mg(ClO_4)_2$ trap was placed after the TPR reactor and before the TCD. In a typical experiment carried out on standard specimens calcined at 650 °C, a 100 mg sample was loaded in a quartz reactor and was flushed with a mixture of H_2 (5%) in Ar at temperatures up to 700 °C, with a ramp of 10 °C/min. Samples were not pre-treated before TPR tests.

Gases evolving from the TPR reactor were analyzed by a Genesys 422 quadrupole mass analyzer (QMS) by a heated capillary. The signals for m/z 34 (H_2S) and 64 (SO_2) were recorded.

Sulphate content was determined by a well-established ion chromatographic method [18].

In-situ FTIR spectra were obtained on a Bruker 113v spectrophotometer (2 cm^{-1} resolution, MCT detector). SZ systems were inspected in the form of thin-layer depositions on a Si platelet (from aqueous suspensions) to obtain information about the powders themselves. FTIR spectra of probe molecules adsorbed thereon were also run, in order to obtain information on surface acidity. Before spectroscopic experiments, all samples were activated in controlled atmosphere at 400 °C in quartz cells (equipped with KBr windows) connected to a conventional high-vacuum line, equipped with coupled rotary and turbomolecular pumps (residual pressure $p < 10^{-5}$ Torr).

2.3. Catalytic tests

The acylation reaction was carried out at 30 °C in a stirred batch reactor with a large excess of aromatic substrate (anisole 10 ml) with respect to both acetic anhydride (278 μl) and catalyst (200 mg). The intra-particle (*i.e.*, pore diffusion) and the external mass transfer effects were avoided by using the catalyst in fine powder form and by employing high stirring speed, respectively.

Before reaction all catalysts were activated at 450 °C in air for 90 min. Gases evolving from the activation reactor were analyzed with the QMS apparatus. The signals for m/z 18 (H_2O), 44 (CO_2), and 64 (SO_2) were recorded.

Upon addition of the reactants, the catalyst (originally white) became pale orange in the colorless solution and deepened to brown-red with reaction time.

Small amounts (100 μl) of the reaction mixture were analyzed after 10, 20, 30, 60, 120 and 180 min by an HP-6890 gas chromatograph equipped with an HP-5 column and a FID detector. GC–MS measurements were performed in order to recognize the metoxyacetophenone isomers and the by-products.

After 3 h the reaction mixture was quickly cooled down, separated from the catalyst, washed with anisole dried at 110 °C and kept for re-usability tests. Exhausted samples were reactivated in air at 450 °C in flowing air. In order to study the carbonaceous species deposited on the catalysts, gases evolving from the reactivation reactor were analyzed with the QMS apparatus. The signals for m/z 18 (H_2O), 43 (CH_3CO)O, 44 (CO_2), 45 (CH_3COOH), and 64 (SO_2) were recorded.

Conversion at time t is calculated on the consumed acetic anhydride (AN_0 represents the initial conversion, whereas AN represents the conversion at time t, and C is referred to the concentration of both species):

$$\text{conversion}\,\% = \frac{C_{AN_0} - C_{AN}}{C_{AN_0}} 100$$

whereas yield is based on the produced metoxyacetophenones (MAP):

$$\text{yield}\,\% = \frac{C_{MAP}}{C_{AN_0}} 100$$

3. Results and discussion

N_2 adsorption/desorption isotherms of all samples are of IV type of the BDDT classification [19], and are characteristic of well-developed mesoporous systems. Hysteresis loops are all of H2–H3 types (see Fig. 1). Mesopores size distribution curves indicate that all samples exhibit a unimodal Gaussian-shaped pore size distribution. BET and BJH characterization data are collected in Table 1. SZA exhibits the smallest specific surface area (SSA), whereas SZF shows the highest SSA and total pore volume. The other samples exhibit a similar (and lower) pore volume.

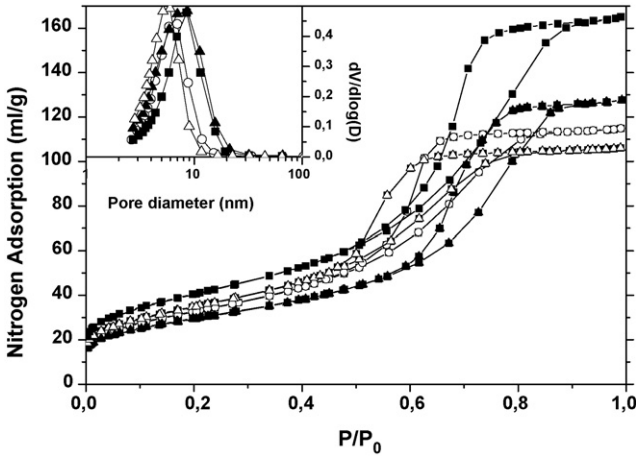

Fig. 1. N_2 physisorption isotherms at −196 °C. Inset: BJH pore size distributions for the four samples. Solid Square: SZF; solid triangle: SZA; open circle: SZ; open triangle: SZG.

Sulphate loading after calcination and the resulting spreading are reported in Table 1. Different samples show different amounts of SO_4 per wt.%, but if the sulphate content is related to the SSA, almost the same number of sulphate groups is obtained (2.1–2.6), ranging in the half-monolayer coverage (~2.5 $SO_4^{=}/nm^2$) [20]. After the 3rd catalytic test, a ~15–20% of SO_4 content was lost (see column 5–6 of Table 1).

X-ray diffraction measurements on fresh calcined catalysts evidence the presence of crystalline ZrO_2 in the tetragonal phase. This is in agreement with the result reported by Canton et al. [21] for SZ promoted with Al_2O_3 and Signoretto et al. [12] for SZ promoted with Ga_2O_3. Al_2O_3 and Ga_2O_3 promoters seem to have a positive effect on the chemical and structural properties of ZrO_2: in particular, they affect the growth of ZrO_2 crystallites modifying the final oxide phase. In fact, the tetragonal form has been reported to be stable (also) in small size crystallites [22].

The reactivity of SZ samples was checked in the acylation of anisole by acetic anhydride to give the corresponding ketones, either 2-or 4-methoxyacetophenone (MOAP), and acetic acid as by-product (see Scheme 1). Moreover, acetic acid can form from the anhydride hydrolysis (acylating agent decomposition, see Scheme 2).

We found for all samples a high selectivity (almost 98–99%) in the *p*-MOAP product. For all catalysts, the production rate of *p*-MOAP is initially very high, but after about 40 min it rapidly decreases, as the anhydride conversion reaches about 60%. The conversion of acetic anhydride (the limiting reagent) to *p*-MOAP reaches about 80% after 3 h.

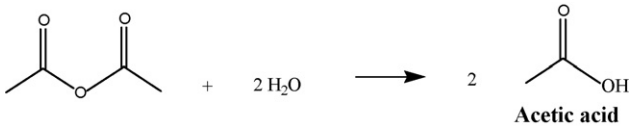

Scheme 2. Acetic anhydride hydrolysis reaction.

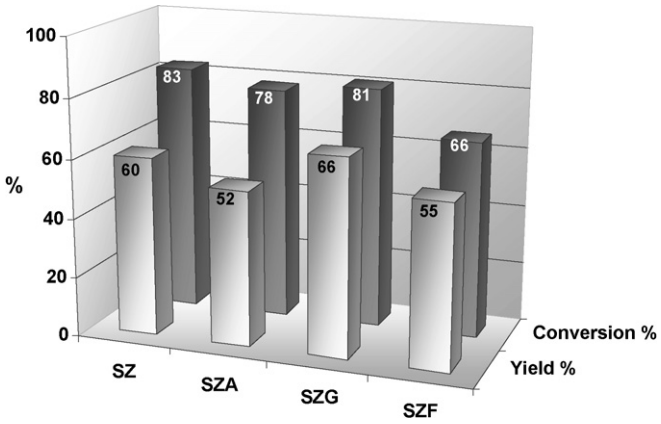

Fig. 2. Conversion vs. yield for all catalysts taken at 3 h of reaction.

A comparison of conversion and yield for all catalysts after 3 h of reaction is reported in Fig. 2. Both plain SZ and SZA catalysts exhibit the largest gap between conversion and yield: this indicates that for these samples the hydrolysis reaction is as significant as the acylation reaction.

Reuse of the catalysts after regeneration is shown in Fig. 3(sections a–d).

Fig. 3a shows conversion and yield for a regenerated SZ catalyst with respect to the fresh one (first run) after 3 h of reaction. Both conversion and yield are not completely restored: they decrease slowly, but with continuity.

For SZA systems (Fig. 3b), an increase of conversion with the number of catalytic runs is observed. This result could be interpreted considering the changes in hydrophilicity of the catalytic surface between each catalytic run and reactivation step. The mass plot of gases evolved during the reactivation step (*i.e.*, activation of the regenerated systems) show that the two main species produced are H_2O and CO_2 (see Fig. 4), whereas no peaks with m/z 43 $(CH_3CO)O$, 45 (CH_3COOH) or 64 (SO_2) were detected. Fig. 4a shows the plots relative to the water removal in the activation step for both fresh and reused catalysts. All fresh catalysts showed only one peak, corresponding to the removal of adsorbed water. The amount of water present in regenerated SZA

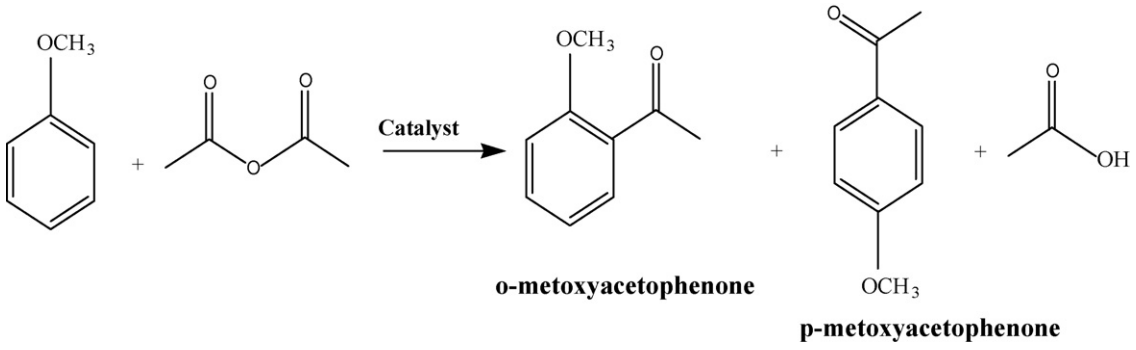

Scheme 1. Acylation of anisole with acetic anhydride.

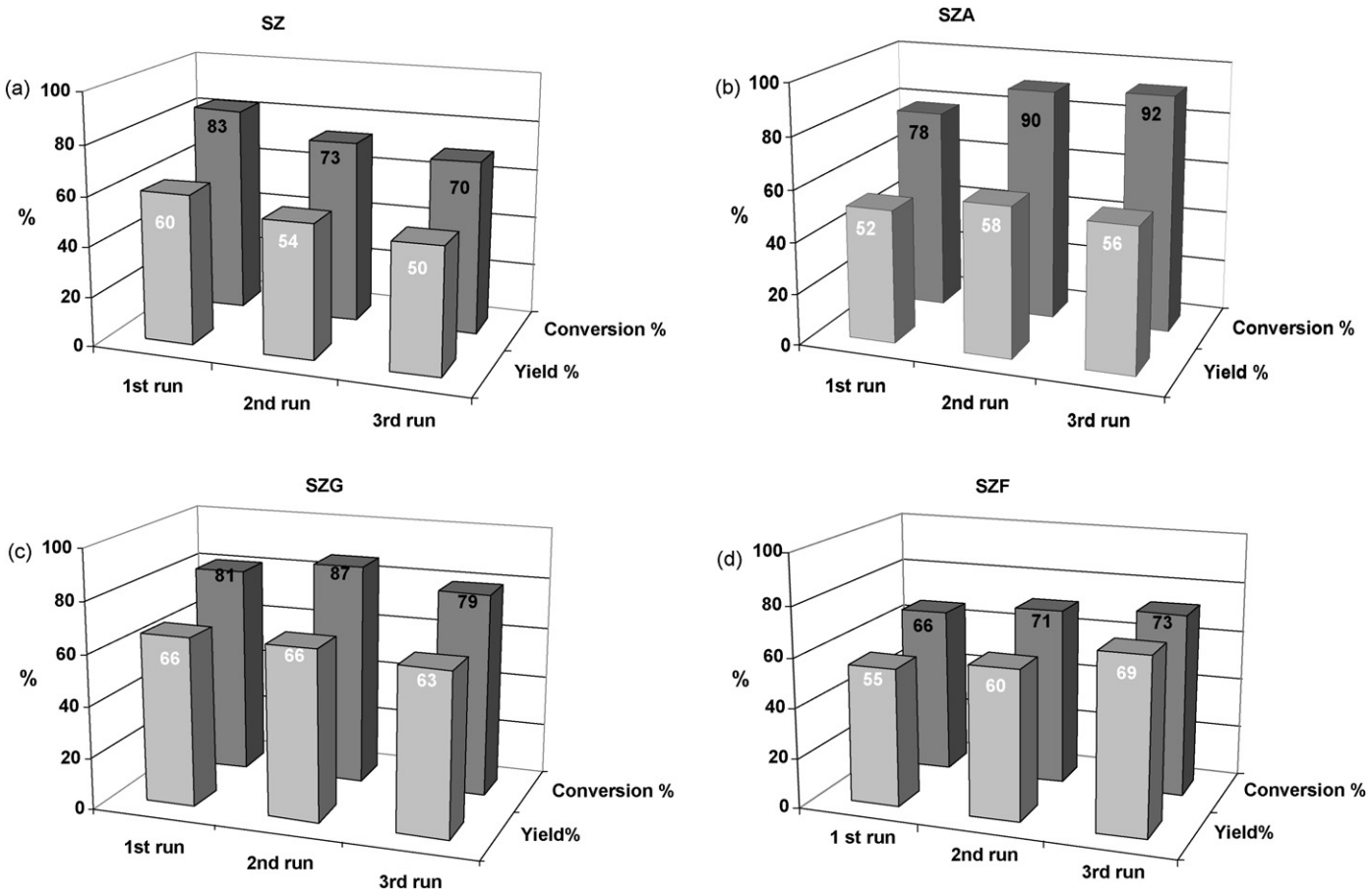

Fig. 3. Reuse of the catalysts after regeneration; (a) SZ, (b) SZA, (c) SZG, and (d) SZF.

samples is higher than in fresh SZA and in all other catalysts. Moreover, it is possible to observe the presence of water at temperature higher than 450 °C, temperature that normally is used in the samples activation, this fact can explain the higher anhydride hydrolysis rate observed for this sample.

For SZG catalysts (Fig. 3c), it was observed that yield and conversion did not change appreciably with regeneration, in fact, in this case the catalyst was found to be completely reusable. Moreover, after reactivation in air at 450 °C, the original white color of the SZG sample was restored. This is not the case for a plain SZ system that, after activation at 450 °C in air, exhibited some gray spots on its surface. Re-activation burnt away most of the carbonaceous residues deposited on the catalyst surface and restored most of the catalyst active sites, but most probably part of the residues remained on the catalyst surface giving rise to an oddly distributed light gray color.

For SZF sample (Fig. 3d), we obtained the best catalytic performances. In fact, in this case not only did the conversion and yield increased with regeneration, but also the gap between them tended to decrease after each use/regeneration cycle. These data seem to indicate that, for the SZF system, the hydrolysis reaction is almost negligible. In fact, the water amount retained after regeneration is appreciably smaller than that of the other catalysts (Fig. 4). Moreover, after regeneration the SZF sample recovered its original color, meaning that during the reactivation process all carbonaceous residues present on the surface were burnt off.

The different trend of the catalysts in the recycling tests could be explained analyzing the mass spectra of CO_2 resulting from the combustion of carbonaceous species deposited on the catalyst surface. As shown in Fig. 4b, the CO_2 peak of SZF and SZG, positioned at 420 and 449 °C, respectively, are shifted to lower temperature if compared to the other samples. (For instance, in the case of the SZA sample, the peak maximum is placed at 464 °C.) These data suggest that Ga_2O_3 and Fe_2O_3 promotion favours the combustion of carbonaceous residues at lower temperatures, so that a regeneration process carried out at 450 °C is sufficient to restore the initial catalytic activity.

In-situ FTIR spectroscopy of basic probe molecules, such as CO and 2,6-dimethylpyridine (lutidine, Lu), adsorbed onto fresh and regenerated SZ systems have been resorted to in order to test their surface acidity. Useful information can be obtained about: (i) strong Lewis acidity, as revealed by CO adsorption at beam temperature (BT), and (ii) total acidity (*i.e.*, Lewis and Brønsted acidity), as revealed by Lu adsorption/desorption in mild conditions.

Fig. 5a reports the IR spectra of CO (100 Torr) adsorbed at BT on fresh promoted and unpromoted SZ systems after activation in vacuo at 400 °C. Only one IR absorption band is always present, centred at ~2198 cm^{-1}. This indicates that CO molecules can interact with only one type of coordinatively unsaturated (cus) surface site. On the basis of both spectral behaviour and literature data [23], the band can be ascribed to the ν_{CO} stretching mode of carbon monoxide adsorbed on a single family of cus Zr^{4+} cations. In this context it is worth recalling that BT uptake of CO onto sulphated *t*-ZrO_2 was found to involve the formation of carbonyl species only with highly uncoordinated Zr^{4+} cations located in the so-called "defective crystallographic positions", such as high-index side terminations of the coin-like crystallites of *t*-ZrO_2 [23b]. Moreover, it is recalled that the presence of surface sulphate species reduces the amount of (strong) Lewis acid centres and

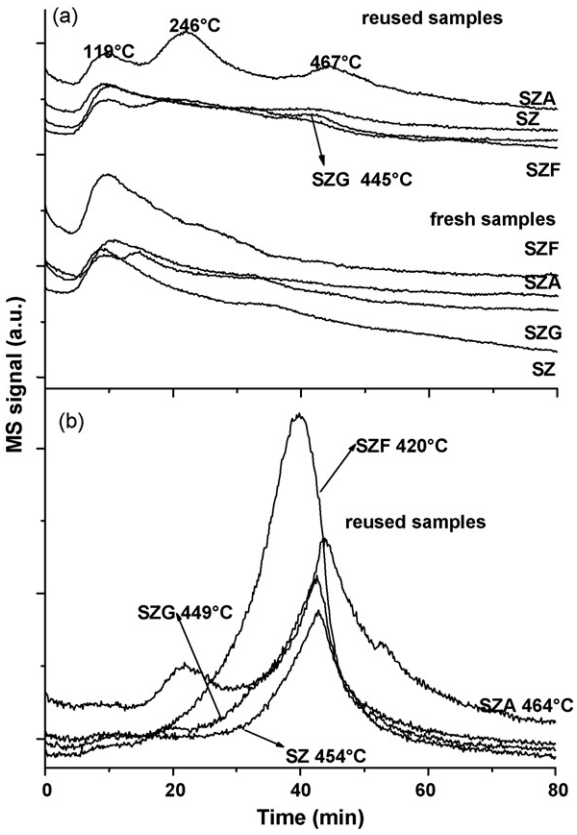

Fig. 4. Mass spectra of water (a) and CO_2 (b) evolved during the activation step. (a) $m/z = 18$, and (b) $m/z = 44$.

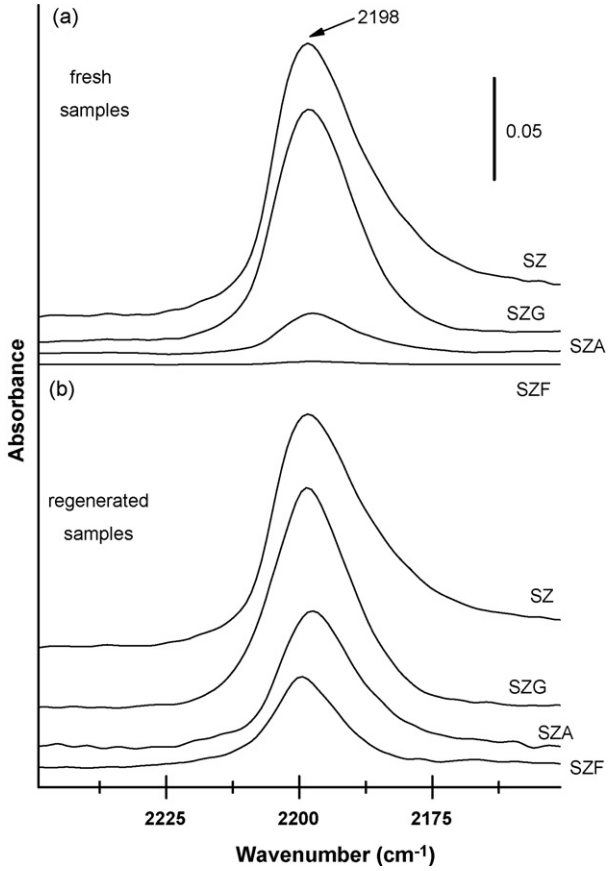

Fig. 5. IR spectra of 100 Torr CO adsorbed at BT on SZ and promoted SZ systems. Section a: fresh catalysts; section b: regenerated catalysts.

modifies only to a rather limited extent the strength of t-ZrO_2 (strong) Lewis acidity [24].

Note that, in the experimental conditions here adopted, no evidence was ever found, in the 2230–2150 cm^{-1} spectral range, for the formation of carbonyl-like bands ascribable to CO interacting with cus Ga^{3+} [25], or Al^{3+} [26], or Fe^{3+} [27] ions. This means that no significant amounts of cationic species other than Zr^{4+} and carrying a high coordinative instauration are present at the surface of the considered SZ systems.

If we consider in more detail the BT interaction of CO with fresh promoted SZ samples, it can be further evidenced that:

(i) in the case of Ga promoted samples (Fig. 5a, curve SZG), there is an almost total spectroscopic coincidence with the unpromoted SZ system (Fig. 5a, curve SZ), and
(ii) for Al promoted sample (Fig. 5a, curve SZA), the amount of strong Lewis acidic sites is very low, whereas in the case of Fe promoted sample (Fig. 5a, curve SZF), no strong cus Zr^{4+} ions are present at the surface in a significant amount.

If CO adsorption is carried out onto regenerated samples (Fig. 5b), some differences are evident. In particular, for both Al and Fe promoted systems the amount of Lewis acidic sites that CO can test at BT is not negligible anymore (see curves SZA and SZF). It is likely that the regeneration procedure sets selected parts of the surface free from some anions (either intrinsic, like OH species, or added, like sulphates), so that an appreciable amount of cationic terminations (*i.e.*, cus Zr^{4+} ions) become now available for interacting with CO molecules. The spectral features of OH and sulphate groups confirm this hypothesis. In fact, if we inspect in some detail the IR spectral ranges in which sulphates and hydroxyl groups absorb (see Fig. 6), the usual spectral patterns are present for the fresh unpromoted SZ system [18,23], as well as for the SZG fresh catalyst (see sections a1 and b1), *i.e.*:

- a strong ν_{OH} band located at ~3650 cm^{-1} (ascribable to tri-bridged surface OH species) with a far less intense component lying at higher frequency (ascribable to terminal OH species) [14]. This is not surprising for a medium-high dehydrated surface on which, upon thermal treatment at 400 °C in controlled atmosphere, OH species have been set free from contaminants (namely, water and carbon dioxide molecules and/or ubiquitous hydrocarbons),
- for what sulphate species is concerned, the "two-bands profile" typical of all catalytically active tetragonal SZ systems [18] is evident, characterized by an intense $\nu_{S=O}$ band at ~1390 cm^{-1} and a partner ν_{S-O} band located at ~1015 cm^{-1}, ascribable to the presence of surface sulphates in a highly covalent form. In addition, a large and unresolved envelope in the 1100–1250 cm^{-1} range is observed, likely to be due to the ν_{S-O} of poly-nuclear surface sulphates [18] and exhibiting a much less relative intensity if compared to the 1390 and 1015 cm^{-1} ν_{S-O} modes.

In the case of Al and Fe promoters (fresh catalysts), the above-described spectral features exhibit some important differences (see sections a1 and b1), as described in the following:

(1) the OH pattern is still characterized by an OH vibration lying at ~3650 cm^{-1}, though far less intense, and (almost) no high-frequency OH component is present. But, most important,

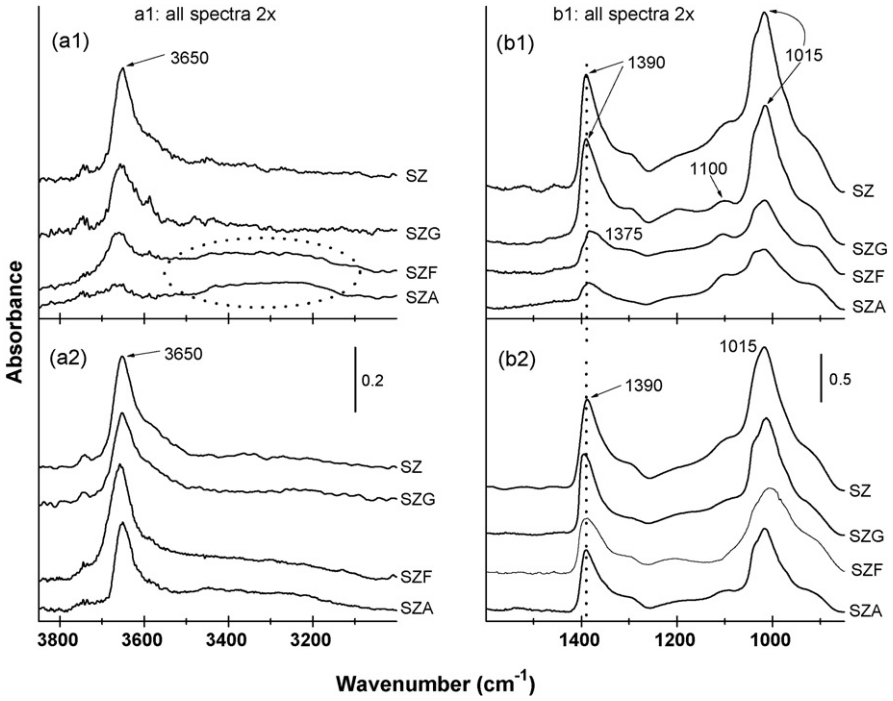

Fig. 6. IR spectra of surface anions (sections a: ν_{OH} region; sections b: ν_{S-O} region) of SZ and promoted SZ systems activated at 400 °C in controlled atmosphere. Section 1 refers to fresh catalysts; section 2 refers to regenerated catalysts.

a broad and unresolved envelope, characterized by a non-negligible intensity (in particular, in the case of SZA systems), is evident in the 3200–3500 cm^{-1} spectral range. On the basis of this spectral behaviour, the latter feature can be ascribed to the presence of surface OH species mutually interacting by H-bonding, still present in spite of the relatively high vacuum activation temperature to which all samples have been subjected. [25];

(2) as for surface sulphates, all of the above described spectral components are present, but the relative intensities of the bands due to the different types of sulphate species turn out to be comparable, meaning that a higher amount of poly-nuclear sulphates still remains at the surface of these materials.

On the contrary, if we compare the spectral features of both OH and sulphates species after regeneration (see sections a2 and b2), it can be noted that in all cases both ν_{OH} and ν_{S-O} modes become better defined, achieving the features of "normal" catalytically active SZ-based materials. In particular, the 3650 cm^{-1} band (in addition to the high-frequency component), typical of free OH

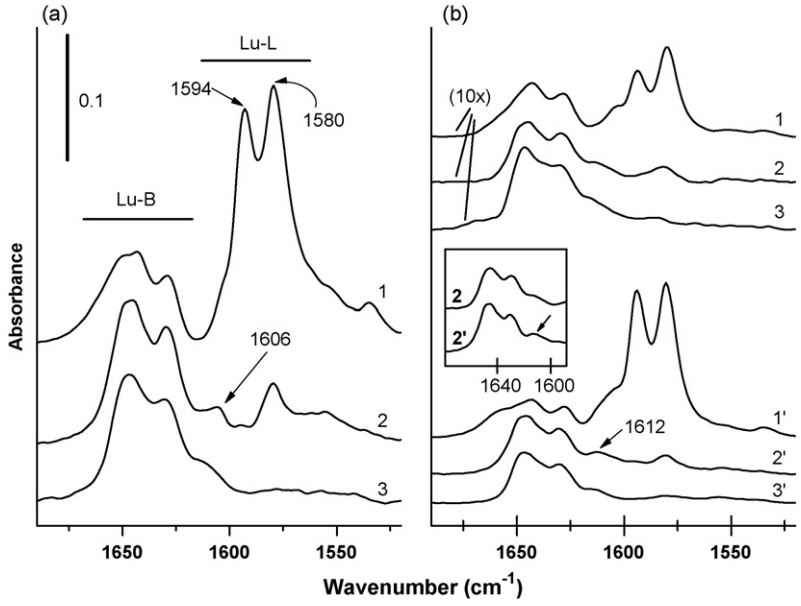

Fig. 7. (a) IR spectra relative to the adsorption/desorption of 2,6-DMP onto a reference SZ system activated in controlled atmosphere at 400 °C. (1) Excess of 2,6-DMP, (2) after evacuation of the base excess at BT, (3) after further evacuation of the base excess at 150 °C. (b) As in section a, adsorption/desorption of 2,6-DMP onto fresh (top spectra, curves 1–3) and regenerated (bottom spectra, curves 1′–3′) SZF samples activated in controlled atmosphere at 400 °C.

groups is now clearly observable for all systems, and (almost) no OH species interacting by H-bonding are now evident anymore (see section a2, curves SZA and SZF). Parallel to this, sulphates groups achieved for all catalysts the typical two-bands profile: this indicated that, during the regeneration process, part of sulphate species decomposed (mainly poly-nuclear sulphates) (see also Table 1), setting a larger portion of the surface either free (so that a larger amount of cus Zr^{4+} cations are now available to coordinate probe molecules like, for instance, CO at BT) or covered by OH groups.

All samples, either fresh or regenerated, were also inspected using the Lu adsorption/desorption procedure [28] after activation in vacuo at 400 °C, in order to test the total presence of Lewis and Brønsted acidity. The spectral features of Lu uptake are reported in Fig. 7a, where only one set of spectra is reported, as all samples exhibited almost the same behaviour.

Protonic (*i.e.*, Brønsted) acidity is always present, as witnessed by the characteristic envelope of bands at $\nu > 1620\ cm^{-1}$ [28]. This is not unexpected in the presence of surface sulphates: in fact, surface anions are known to induce protonic acidity at the surface of pure oxides [29]. Other bands are also evident at $\nu < 1620\ cm^{-1}$. In particular, if the spectrum is obtained in the presence of an excess of Lu (Fig. 7a, curve 1), the usual two-bands profile of scarcely perturbed Lu is observed [28]. These main peaks, centred at ~1580 and ~1594 cm^{-1}, are ascribed to physisorbed and H-bonded Lu species, respectively, whereas a shoulder at higher ν(~1605–1615 cm^{-1}) is ascribable, when present, to the 8a mode of a more severely perturbed Lu species, *i.e.*, to Lu species Lewis-coordinated at cus Zr^{4+} cations (Lu-L) [28].

Upon evacuation of the base excess at BT (Fig. 7a, curve 2) some important features can be evidenced:

(i) the overall intensity of the envelope located at $\nu < 1620\ cm^{-1}$ is drastically decreased, as expected of H-bonded and physisorbed weakly bound species. Within the remaining envelope, a band centred at ~1605–1610 cm^{-1}, due to the 8a mode of Lewis-coordinated Lu, is now quite evident, and
(ii) unlike that, the broad envelope located at $\nu > 1620\ cm^{-1}$ (due to Brønsted-bound Lu species, Lu-B) turns out to be little affected by the evacuation, if at all, as it remains strong and complex as it was before evacuation. Even if the evacuation of the base is carried out at 150 °C (Fig. 7a, curve 3), the bands due to Lu-B remain almost unaltered, while the residual concentration of the aprotic fraction becomes negligible.

In the case of the SZF system some differences are evident between the fresh and the regenerated samples. Fig. 7b reports the spectral features relative to the adsorption/desorption of Lu onto fresh (top spectra, curves 1–3) and regenerated (bottom spectra, curves 1′–3′) SZF materials, after activation at 400 °C.

The main Lu bands, described and assigned in the above section, are still present, but:

(i) the relative intensity of the Lu-L fraction ($\nu < 1620\ cm^{-1}$) with respect to the Lu-B one ($\nu > 1620\ cm^{-1}$) is very different. In fact, in the case of a fresh SZF sample, a ~1:1 ratio is observed, whereas for the regenerated catalyst the Brønsted-bound envelope exhibits a much lower relative intensity: this is likely to be due to the loss of part of sulphate groups, which are known to be primarily responsible for protonic acidity, and
(ii) as a consequence of sulphates decomposition, a higher amount of cus cations is now available at the surface and capable to interact with basic probe molecules: in the inset of Figure 7b, the arrow indicates the band due to Lu-L strongly interacting with Zr^{4+} sites. Its presence is definitely better defined in the case of the regenerated SZF catalyst (curve 2'). Note that this aspect is consistent with what clearly indicated, in a previous section, by CO adsorption at BT (see the SZF curves in Fig. 5)

The increase of catalytic activity for SZF samples, before and after regeneration, can be in part ascribed to a modification of their acidity. The regenerated sample is likely to develop a strong Lewis acidity (mostly or) only after reactivation, and this might be due to the partial elimination of surface sulphates (*vide infra* and Table 1). In fact, the presence of a larger amount of surface sulphate species reduces the possible amount of coordinatively unsatured Zr^{4+} cations and the possibility of their interaction basic probe molecules.

It has been observed that, during the reactivation step, part of sulphates were eliminated as SO_2, even in oxidizing conditions, and this aspect was particularly evident in the case of SZF samples. These data were confirmed by IC on reused samples, which showed a big loss of SO_4 species from SZF and SZG samples (see Table 1).

Fig. 8 shows the TPR profiles in the 30–700 °C temperature range (plots in the central picture) and the MS spectra (insets a–d, m/z 34 and m/z 64) for all fresh samples. The TPR profile of the SZ sample displayed only one strong and sharp peak, starting at 500 °C and peaking at 650 °C. Blank experiments on *t*-ZrO_2 and *m*-ZrO_2 (not shown) confirmed the absence of TPR peaks in this temperature region for non-sulphated systems. The mentioned peak must be therefore assigned to the reduction of S(VI) species, as already reported by other authors [30–32].

For SZA catalysts a single reduction peak with maximum at 680 °C was observed. On the other hand, for SZG catalysts two reduction peaks were observed: the first one, quite asymmetric on the low-T side, is placed at relatively low temperatures (530 °C), whereas the second peak (~550 °C) is superimposed on the main one, as a sort of high-temperature shoulder.

For SZF samples only one reduction peak was observed, located at relatively low temperature with an asymmetric maximum centred at ~460 °C. This indicates that, on both SZG and SZF samples, the reduction of S(VI) species occur at lower temperatures than on either plain SZ or SZA materials. The presence of Ga_2O_3 and Fe_2O_3 in crystalline *t*-ZrO_2 systems rendered surface sulphate species far more readily reducible.

Mass spectrometry (MS) data of Fig. 8(a–d) indicate that for all samples two products result from sulphates reduction and namely as SO_2 and H_2S. Still, the two products did not evolve in parallel in the whole temperature range, as initially only SO_2 formed. For both unpromoted and Al-promoted SZ samples the first major peak is placed at 450–650 °C with maximum yield at ~640 °C and is due at SO_2, beyond 600 °C, H_2S evolution is observed, but this peak is very small and superimposed. For Ga_2O_3- and Fe_2O_3-promoted samples MS analysis shows two distinct features a low-temperature peak related to SO_2 formation (the peak is centred at 490 °C for GSZ and at 440 °C for FSZ samples), followed by a higher temperature peak related to H_2S formation.

In both SZG and SZF systems there is an evident lowering of sulphates reduction temperatures with respect to SZ and SZA samples: this feature may indicate that Ga_2O_3- or Fe_2O_3-promoted samples possess enhanced red-ox properties.

The characterization data seem to indicate the possible effect of these red-ox properties in the regeneration step. Possibly, samples promoted with Ga and Fe oxides are able to favour the oxidation (or burn-off) of the adsorbed species on catalytic surface and either to allow a better cleaning process or to lead to further sulphate removal.

Moreover in these systems the elimination of sulphate species at lower temperature sets free cus Zr cations, and brings a change (enhancement) of catalyst acidity.

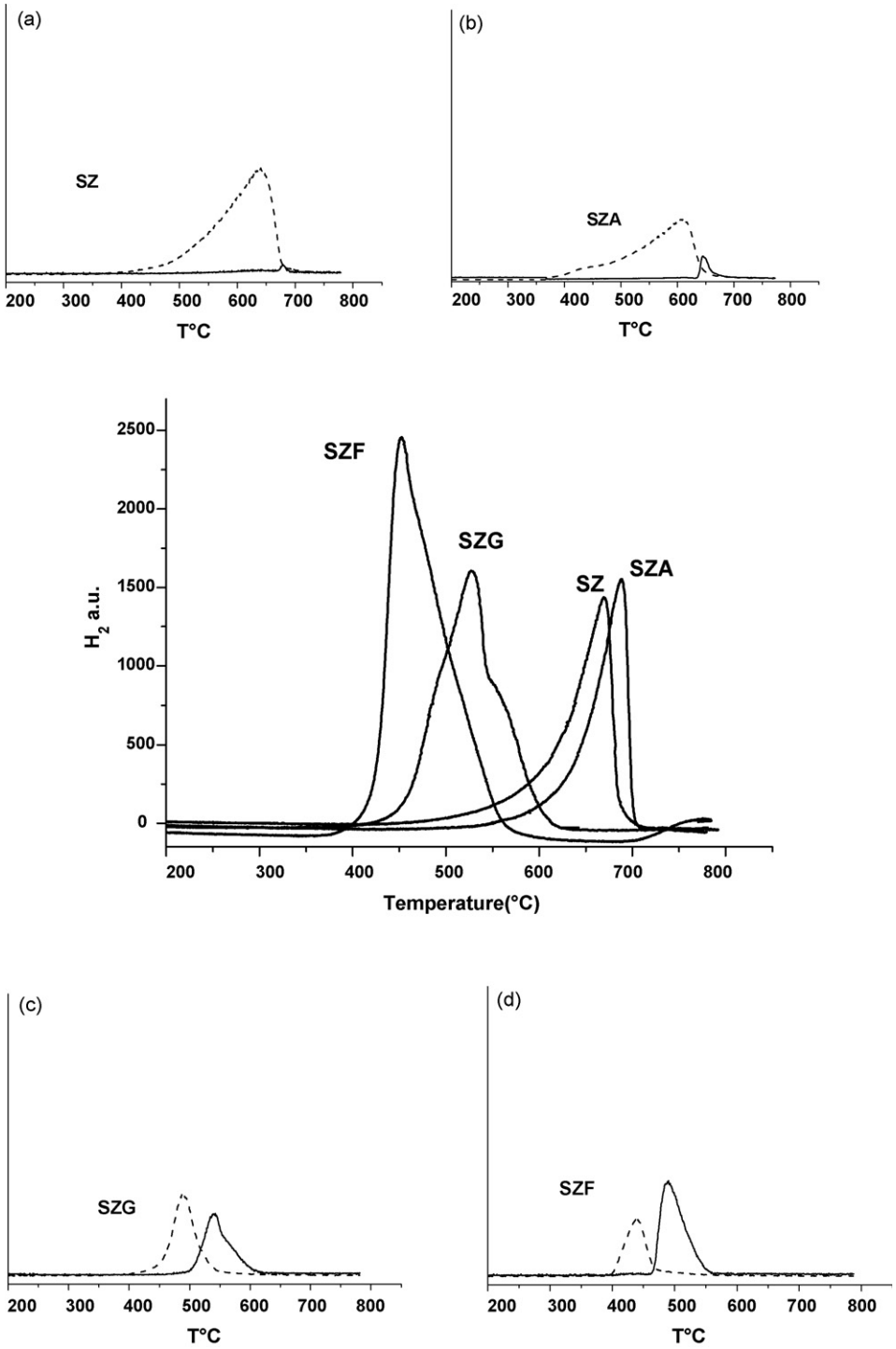

Fig. 8. (Central plot): TPR analysis profiles, (a–d) mass spectra of the gases evolved during the TPR analyses, solid line: $m/z = 34$, broken line $m/z = 64$,

4. Conclusions

High conversion and *p*-selectivity in the acylation reaction of anisole with acetic anhydride were achieved in the presence of SZ promoted catalysts under mild reaction conditions. The catalytic activity (yield) is strongly influenced by of the hydration grade of the surface.

Deactivation during the acylation reactions can be attributed to reversible effects. These might lead to an unusual ratio between Lewis and Brønsted acid sites, *i.e.*, to either the formation of carbonaceous deposits at the surface of the catalyst or to higher hydration degree of the surface itself. It is possible to regenerate the catalysts after burning off (this process implies also the removal of water, if present) the carbonaceous residues deposited on the catalyst surface, and this process is easier for either Fe or Ga promoted samples. The better performance after regeneration for these samples can be then explained in term of enhanced red-ox properties, which allow the complete restoration of the catalytic activity at lower temperature than in the other cases (either non-promoted or Al-promoted SZ catalysts).

Acknowledgments

The financial supports from MURST (Project FIRB-2001) and INSTM (PRISMA Project) are gratefully acknowledged.

References

[1] H.W. Kouwenhoven, H. van Bekkum, in: G. Ertl, H. Knoetzinger, J. Weitkamp (Eds.), Handbook of Heterogeneous Catalysis, 5, Wiley-VCH, Weinheim, 1997, p. p.2358.
[2] G.A. Olah, Friedel-Crafts and Related Reactions, Wiley, New York, 1973.
[3] A. Corma, M.J. Climent, H. Garcia, J. Primo, Appl. Catal. 49 (1989) 109.
[4] D. Rohan, C. Cnaff, E. Formentin, M. Guisnet, J. Catal. 177 (1998) 296.
[5] B.M. Choudary, M. Sateesh, M.L. Kantam, K.V.R. Prasad, Appl. Catal. A 171 (1998) 155.
[6] P. Metivier, in: R.A. Sheldon, H. van Bekkum (Eds.), Fine Chemicals through Heterogeneous Catalysis, Wiley, Weinheim, Toronto, 2001, p. 161.
[7] M. Spagnol, L. Gilbert, E. Benazzi, C. Marcilly, Patent to Rhodia WO 96/35655. (1996).
[8] M. Guidotti, C. Canaff, J.-M. Coustard, P. Magnoux, M. Guisnet, J. Catal. 230 (2005) 375.
[9] E.G. Derouane, C.J. Dillon, D. Bethell, S.B. Derouane-Abd Hamid, J. Catal. 187 (1999) 209.
[10] S.K. Jana, Catal. Surv. Asia 9 (1) (2005).
[11] S. Melada, M. Signoretto, F. Somma, F. Pinna, G. Cerrato, G. Meligrana, C. Morterra, Catal. Lett. 94 (2004) 193.
[12] M. Signoretto, S. Melada, F. Pinna, S. Polizzi, G. Cerrato, C. Morterra, Micropor Mesopor Mat. 81 (2005) 19.
[13] G.K. Chuah, S. Janeicke, S.A. Cheong, K.S. Chan, Appl. Catal. A 145 (1996) 267.
[14] K.T. Jung, A.T. Bell, J. Mol. Catal. A 163 (2000) 27.
[15] M.A. Risch, E.E. Wolf, Appl. Catal. A 172 (1998) L1–L5.
[16] S.J. Gregg, K.S.W. Sing, Adsorption Surface Area and Porosity, second ed., Academic Press, Inc., 1982.
[17] E.P. Barret, L.G. Joyner, P.P. Halenda, J. Am. Chem. Soc. 73 (1951) 373.
[18] C. Sarzanini, G. Sacchero, F. Pinna, M. Signoretto, G. Cerrato, C. Morterra, J. Mater. Chem. 5 (1995) 353.
[19] S. Brunauer, L.S. Deming, W.S. Deming, E. Teller, J. Am. Chem. Soc. 62 (1940) 1723.
[20] P. Nascimento, C. Aktatopoulou, M. Oszagyan, G. Coudrier, C. Travers, J.F. Joly, J.C. Vedrine, in: L. Guczi, F. Solymosi, P. Tetenyi (Eds.), New Frontiers in Catalysis, Elsevier Science Publisher B.V, 1993, p. 1185.
[21] P. Canton, R. Olindo, F. Pinna, G. Strukul, P. Riello, M. Meneghetti, G. Cerrato, C. Morterra, A. Benedetti, Chem. Mater. 13 (2001) 1634.
[22] R.C. Garvie, J. Phys. Chem. 69 (1965) 1238.
[23] (a) G. Herzberg, Molecular Spectra and Molecular Structure. II. Infrared and Raman Spectra of Polyatomic Molecules, Van Nostrand Co., New York, 1947, p. 274;
(b) C. Morterra, G. Cerrato, V. Bolis, S. Di Ciero, M. Signoretto, J. Chem. Soc., Faraday Trans. 93 (1997) 1179;
(c) W. Stichert, F. Schüth, S. Kuba, H. Knözinger, J. Catal. 198 (2001) 277.
[24] C. Morterra, G. Cerrato, C. Emanuel, V. Bolis, J. Catal. 142 (1993) 349.
[25] (a) M. Rodrìguez Delgado, C. Morterra, G. Cerrato, G. Magnacca, C. Otero Areàn, Langmuir 18 (2002) 10255;
(b) G. Cerrato, C. Morterra, M. Rodrìguez Delgado, C. Otero Areàn, M. Signoretto, F. Somma, F. Pinna, Micropor Mesopor Mat. 94 (2006) 40.
[26] C. Morterra, G. Magnacca, Catal. Today 27 (1996) 497.
[27] A. Zecchina, D. Scarano, A. Reller, J. Chem. Soc., Faraday Trans. I 84 (7) (1988) 2327.
[28] C. Morterra, G. Meligrana, G. Cerrato, V. Solinas, E. Rombi, M.F. Sini, Langmuir 19 (2003) 5344.
[29] T. Yamaguchi, Appl. Catal. 61 (1990) 1.
[30] A. Sayari, A. Dicko, J. Catal. 145 (1994) 561.
[31] A. Dicko, X. Song, A. Adnot, A. Sayari, J. Catal. 150 (1994) 254.
[32] B.-Q. Xu, W.M.H. Sachtler, J. Catal. 167 (1997) 224.